Critical slowing down in driven-dissipative Bose-Hubbard lattices

Filippo Vicentini, Fabrizio Minganti, Riccardo Rota, Giuliano Orso, and Cristiano Ciuti[*]
*Laboratoire Matériaux et Phénomènes Quantiques, Université Paris Diderot, Sorbonne Paris Cité,
UMR No. 7162, CNRS, 75013 Paris, France*

We explore theoretically the dynamical properties of a first-order dissipative phase transition in coherently driven Bose-Hubbard systems, describing, e.g., lattices of coupled nonlinear optical cavities. Via stochastic trajectory calculations based on the truncated Wigner approximation, we investigate the dynamical behavior as a function of system size for one-dimensional (1D) and 2D square lattices in the regime where mean-field theory predicts nonlinear bistability. We show that a critical slowing down emerges for increasing number of sites in 2D square lattices, while it is absent in 1D arrays. We characterize the peculiar properties of the collective phases in the critical region.

I. INTRODUCTION

In a closed many-body quantum system at zero temperature, the pure ground state may undergo a quantum phase transition when there is a competition between two physical processes described by noncommuting Hamiltonian terms [1]. In an open system [2], the competition between unitary Hamiltonian evolution and dissipation can induce a dissipative phase transition for the steady state in the thermodynamic limit [3], as it has been discussed theoretically for photonic systems [4–13], lossy polariton condensates [14–16], and spin models [17–21].

Photonic systems are particularly promising to investigate dissipative phase transitions described by Bose-Hubbard-like models [22–25], particularly in platforms based on patterned semiconductor microcavities [26] and nonlinear superconducting microwave resonators [27–29]. A few interesting experiments on photonic systems have been reported recently, such as a spectroscopic and dynamical study of a one-dimensional array where the first resonator is coherently pumped [28] and the observation of a dissipative phase transition in a coherently driven semiconductor micropillar [30,31] or in a single superconducting nonlinear resonator [32]. The field is still in its infancy, but comprehensive experimental investigations of controlled one- and two-dimensional [26] nonlinear photonic lattices are within reach.

In a lattice of coupled resonators with local boson-boson interaction U a coherent and homogeneous driving of all the sites can create a macroscopic population of bosons in the zero-wave-vector mode ($k = 0$). Being delocalized in space, the latter experiences a self-interaction of strength U/N, N being the number of sites. If one retains only the $k = 0$ mode operators in the driven-dissipative Bose-Hubbard model, such crude approximation predicts a first-order phase transition for a critical driving strength [9]. An interesting and challenging problem is to understand how the presence of the other modes with $\mathbf{k} \neq \mathbf{0}$ affects the dynamics of the system. In particular, the emergence of criticality might depend on fluctuations associated with this multitude of modes and on the dimensionality of

the lattice. A recent work [10] has reported calculations of the steady-state population for lattices as a function of the driving strength, suggesting the presence of a first-order discontinuity in two-dimensional lattices, but only a smooth crossover in one-dimensional arrays.

The finite-size scaling of the dynamical properties have not been systematically explored in driven-dissipative lattice systems. This is a challenging theoretical problem because it requires the study of a large number of modes and very long time scales. In equilibrium systems, a critical slowing down of transient dynamics is observed at the critical point when the Hamiltonian energy gap vanishes. Instead, in dissipative systems a critical slowing down is expected to be related to the spectrum of the Liouvillian superoperator governing the time evolution of the density matrix [3]. However, a clear demonstration of critical slowing down as a function of lattice size is still missing.

In this paper we explore the dynamical properties of the driven-dissipative Bose-Hubbard model in both one-dimensional (1D) and 2D square lattices. Within the truncated Wigner approximation, we solve stochastic Langevin equations for the lattice fields and determine the dependence of relaxation time dynamics towards the steady state as a function of lattice size. We are able to determine the presence of critical slowing down in 2D lattices due to the emergence of a first-order phase transition between a collective low-density and high-density phase. We characterize this paradigm of dissipative phase transition via a comprehensive study of the main observables.

II. THEORETICAL FRAMEWORK AND METHODS

The Bose-Hubbard model in the presence of coherent driving with frequency ω_p is described by the Hamiltonian (in the frame rotating with the drive $\hbar = 1$)

$$\hat{H} = \sum_j -\Delta \hat{a}_j^\dagger \hat{a}_j + \frac{U}{2} \hat{a}_j^{\dagger 2} \hat{a}_j^2 + F(\hat{a}_j^\dagger + \hat{a}_j) - J \sum_{\langle j,j' \rangle} \hat{a}_j^\dagger \hat{a}_{j'},$$

(1)

_____
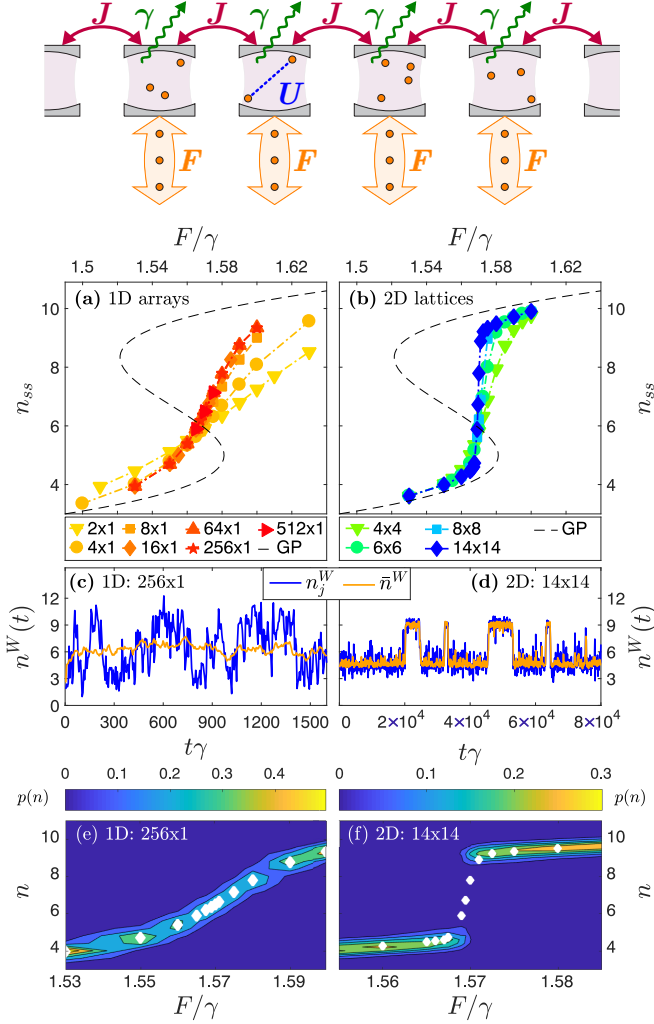[*]cristiano.ciuti@univ-paris-diderot.fr

FIG. 1. Depicted on top is the considered driven-dissipative Bose-Hubbard system (only the 1D case is shown): The left panels are for 1D arrays, while the right panels refer to 2D square lattices. (a) and (b) Steady-state average population per site versus driving amplitude F (in units of the dissipation rate γ) for lattices of different size. The dashed line is the prediction of the Gross-Pitaevskii mean-field theory. (c) and (d) Time-dependent single-trajectory population n_j^W in the jth site (dark blue) and the same quantity averaged over all sites $\bar{n}_j^W$ (light orange) for $F = 1.5695\gamma$. (e) and (f) Contour plot of the probability distribution $p(n)$ of the site-averaged steady-state population versus the driving. White diamonds represent the steady-state average population per site, also shown in (a) and (b). (c) and (e) are for a 256×1 array, while (d) and (f) are for a 14×14 lattice. Trajectories have been computed via the truncated Wigner approximation with the parameters $U = 0.1\gamma$, $\Delta = 0.1\gamma$, and $zJ = 0.9\gamma$ (hopping rate times the coordination number z).

where $\Delta = \omega_p - \omega_c$ is the detuning between the driving frequency and mode frequency ω_c, U the on-site interaction, F the homogeneous driving field (the phase is chosen in such a way that F is real), and J the hopping coupling between two nearest-neighbor sites (see Fig. 1, top panel). In the following, z will denote the number of nearest neighbors ($z = 2$ and $z = 4$, respectively, for the 1D and 2D lattices considered in this work). To describe the dissipative dynamics, we will consider

the following Lindblad master equation for the lattice reduced density matrix $\hat{\rho}$, assuming a uniform Markovian single-boson loss rate γ [2]:

$$\frac{\partial \hat{\rho}}{\partial t} = \mathcal{L}\hat{\rho} = -i[\hat{H}, \hat{\rho}] + \frac{\gamma}{2} \sum_j [2\hat{a}_j \hat{\rho} \hat{a}_j^\dagger - \{\hat{a}_j^\dagger \hat{a}_j, \hat{\rho}\}]. \quad (2)$$

The Liouvillian non-Hermitian superoperator $\mathcal{L}$ has a complex spectrum of eigenvalues $\{\lambda_r\}$ with $\text{Re}(\lambda_r) \leqslant 0$, defined by the eigenvalue equation $\mathcal{L}\hat{\rho}_r = \lambda_r \hat{\rho}_r$. The steady state is usually unique [33] and corresponds to the zero eigenvalue. The real part of the nonzero eigenvalues is responsible for the transient relaxation of the density matrix to the nonequilibrium steady state $\hat{\rho}_{ss}$. The slowest relaxation dynamics is due to the eigenvalue with the smallest real part (in absolute value). We call $\lambda = \min_r |\text{Re}(\lambda_r)|$ the Liouvillian frequency gap, which is the inverse of the asymptotic decay rate towards the steady state. A dissipative phase transition is expected to be characterized by a critical slowing down associated with the closing of the Liouvillian gap in the thermodynamic limit [3].

In this work we explore lattices in a regime where the so-called truncated Wigner approximation method can be applied [22,34,35]. In general, the Lindblad master equation can be mapped exactly into a third-order differential equation for the quasiprobability Wigner function, which is a representation of the density matrix. In the limit of small U, the third-order derivatives can be neglected so that the differential equation (2) becomes a Fokker-Planck equation [36] for a well-defined probability function [22,34]. The latter can be solved via a stochastic Monte Carlo approach [37] described by a set of Langevin equations for the complex field $\alpha_j(t)$ of the boson mode in the jth site:

$$\dot{\alpha}_j = \{-i[\Delta - U(|\alpha_j|^2 - 1) - \gamma/2]\}\alpha_j$$
$$- iJ \sum_{j'} \alpha_{j'} + iF + \sqrt{\gamma/2}\chi(t), \quad (3)$$

where j' runs over the nearest neighbors of j and $\chi(t)$ is a normalized random complex Gaussian noise such that $\langle \chi(t)\chi(t')\rangle = 0$ and $\langle \chi(t)\chi^*(t')\rangle = \delta(t - t')$. Within this formalism, expectation values for symmetrized products of operators [22,34] are obtained by averaging over different stochastic trajectories through the relation $\langle\{(\hat{a}_i^\dagger)^n, \hat{a}_j^m\}_s\rangle = \frac{1}{N_{\text{traj}}} \sum_r (\alpha_{i,r}^*)^n \alpha_{j,r}^m$, where the index r runs over the N_{traj} random trajectories.

III. RESULTS

Here we will explore the driven-dissipative Bose-Hubbard model and investigate a first-order phase transition in a regime where mean-field theory predicts bistability. Within a Gross-Pitaevskii-like mean-field approach [38], the master equation for the lattice density matrix is replaced by a simple equation for the mean field $\alpha_j = \langle \hat{a}_j \rangle$, which is the same as Eq. (3), but without the noise terms. In the homogenous case ($\alpha_j = \alpha$), the steady-state equation takes the nonlinear form $|\alpha|^2[(\Delta + zJ - U|\alpha|^2)^2 + \gamma^2/4] = F^2$, which can have three nondegenerate solutions for a given F, two of which are dynamically stable. As in all mean-field theories [11,38,39], the effect of hopping depends only on zJ, with the lattice dimension playing no role. Hence, in the following, when comparing 1D versus

2D lattices, we will consider the same value of zJ so that differences will only be due to effects beyond mean field.

In Fig. 1(a) we present results obtained with the truncated Wigner approximation for the steady-state site-averaged population $n_{ss} = \frac{1}{N} \sum_{i=1}^{N} \text{Tr}(\hat{\rho}_{ss} \hat{a}_i^\dagger \hat{a}_i)$ for 1D arrays of different length L (up to $L = 512$). In Fig. 1(b) the same observable is reported for 2D $L \times L$ lattices (up to 14×14). Both 1D and 2D calculations have been performed with periodic boundary conditions. For the value $U = 0.1\gamma$ considered in the following, we have successfully benchmarked (see the Appendix) the accuracy of the truncated Wigner approximation for small lattices by comparison with brute-force numerical integrations of the master equation and also calculations based on the corner-space renormalization method [40]. In both Figs. 1(a) and 1(b) the Gross-Pitaevskii-like mean-field prediction is depicted by the dashed line. While, in general, mean-field theories exhibit multistability, the density-matrix solution of the master equation is, under quite general assumptions, unique [33,41]: Indeed, quantum fluctuations make the mean-field solutions metastable so that on a single trajectory the system switches back and forth from one metastable state to another on a time scale related to the inverse Liouvillian gap [6,30,34,42] [see also Fig. 1(c)]. The results in Fig. 1(a) show that the S-shaped multivalued curve of the mean-field theory is replaced by a single-valued function, which depends on the array size L. Remarkably, by increasing the size L of the array $n_{ss}(F)$ eventually converges to a curve with a finite slope. On the other hand, in two dimensions the slope of $n_{ss}(F)$ does not saturate when increasing the size L of the lattices, suggesting the emergence of a discontinuous jump in the thermodynamic limit compatible with a first-order phase transition.

In Figs. 1(c) and 1(d) we present the dynamics of the boson population in a single stochastic Wigner trajectory for the 1D and 2D lattices, respectively. In the considered regime of interaction U, Wigner trajectories have a direct correspondence to local oscillator measurements [43], such as those carried out via homodyne detection techniques [44,45]. In one dimension, switches between the two metastable mean-field solutions are barely visible in the population of the jth site $n_j^W(t)$ (blue curve) and are absent in the site-averaged population $\bar{n}^W(t) = 1/N \sum_{j=1}^{N} n_j^W(t)$ (orange curve), consistent with the formation of moving domains with low and high density inside the array [10]. On the contrary, the 2D lattice exhibits a strikingly different behavior, with a clear random switching behavior of $n_i^W(t)$ between two well-defined metastable states. The populations in all sites switch collectively since $n_j^W(t)$ and $\bar{n}^W(t)$ strongly overlap. Furthermore, notice that the 2D time scales are far longer than in the 1D case, indicating a significantly slower dynamics. A particularly insightful quantity is the probability number distribution $p(n)$ defined as follows. We consider a time t_s where the system has reached the steady state and statistically collect all the values of $n = \bar{n}^W$ ($t > t_s$) for all the considered trajectories. The results for $p(n)$ are presented in Figs. 1(e) and 1(f) for different values of the driving amplitude F. We notice that, in the 1D case, this distribution is monomodal for all values of F and the steady-state mean value of the population follows the peak of this distribution. In the 2D lattice $p(n)$ exhibits a completely different behavior: It has a single peak in the limit of small and large F, while it
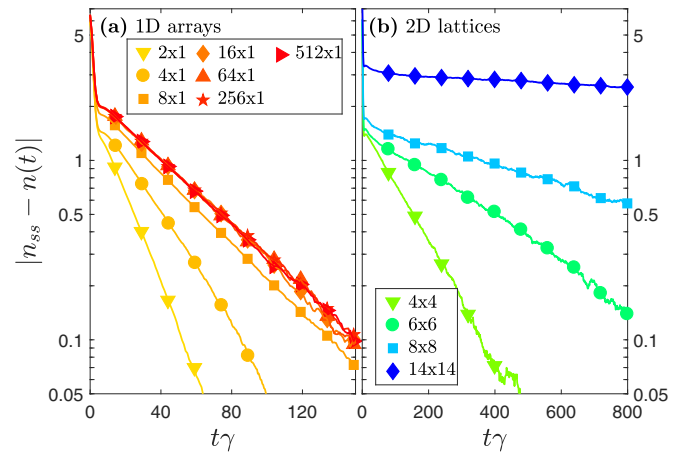

FIG. 2. Transient dynamics of the absolute difference between the mean occupation number $n(t)$ and its steady-state value n_{ss} for (a) 1D arrays and (b) 2D lattices of different sizes, with driving amplitude $F = 1.57\gamma$. Other parameters are as in Fig. 1.

is bimodal in proximity of the critical region. Here, for finite size the steady-state expectation value n_{ss} falls in a region of negligible probability [$p(n_{ss}) \simeq 0$] in between two peaks corresponding to the low- and high-population phases. When the 2D lattice size is increased, the crossover between the two phases becomes steeper and therefore the bistable region also becomes narrower, eventually collapsing to a single point when $L \to \infty$. This explains why in large lattices a fine scan in F is necessary to observe this feature.

To investigate the emergence of criticality in the dynamical properties, we calculated the time evolution towards the steady-state value n_{ss} of the site-averaged mean occupation number $n(t) = \frac{1}{N} \sum_{i=1}^{N} \text{Tr}(\hat{\rho}(t) \hat{a}_i^\dagger \hat{a}_i)$, taking the vacuum as initial state. For values of F close to the critical point, $n(t) - n_{ss}$ decays exponentially to zero at large times as reported in Fig. 2. In this asymptotic regime, the dynamics is dominated by the Liouvillian gap λ, which can be extracted by fitting the results with $n(t) = n_{ss} + A e^{-\lambda t}$. Note that in order to have enough accuracy, calculations have required up to 10^6 stochastic Wigner trajectories for each data point. Experimentally, the asymptotic decay rate can be also measured using the time dependence of the second-order correlation function [31], dynamical optical hysteresis [30], and switching statistics [28,30]. The particular case of $F = 1.57\gamma$ is analyzed in Fig. 2, where we plot $|n_{ss} - n(t)|$ for 1D arrays [Fig. 2(a)] and 2D lattices [Fig. 2(b)] of different sizes. For this fixed value of F, the dynamics gets slower as the size of the simulated system is increased. While in the 1D case the exponential decay rate saturates in the thermodynamic limit, this is not the case for 2D systems. The emergence of critical slowing down is quantified in Fig. 3, where we provide the size dependence of the Liouvillian gap λ versus F. In Fig. 3(a) we report results for 1D arrays: It is apparent that, when the size L is large enough, the Liouvillian gap converges to a finite value for all the values of F, thus proving the absence of critical slowing down. The behavior is strikingly different for 2D lattices, as shown in Fig. 3(b): In this case, every curve $\lambda(F)$ presents a minimum, which becomes smaller and smaller when the size L of the lattice is increased. As shown in the inset of Fig. 3(b), the minimum of λ follows the power-law
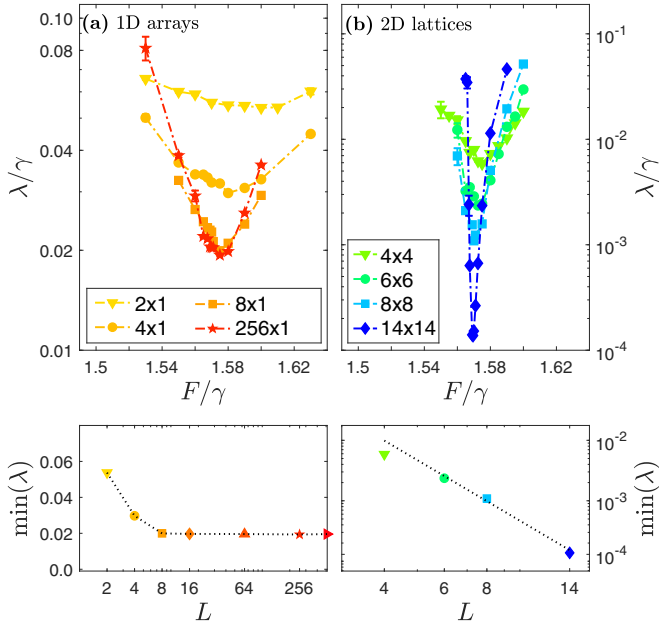
FIG. 3. Liouvillian gap λ (logarithmic scale) versus the driving amplitude for several (a) $L \times 1$ arrays and (b) $L \times L$ lattices. Notice the different scales used for the 1D and 2D cases. The insets show the minimum of λ as a function of the size L. Error bars are within the symbol size. Parameters are as in Fig. 1.

decay $\min_\lambda(L) \propto L^{-\eta}$, with exponent $\eta = 3.3 \pm 0.1$. Since the phase transition is of first order, this exponent is not universal [9,31]. To verify this, we computed the critical exponent in lattices with a different nonlinearity (the other parameters were unchanged), finding $\eta = 5.3 \pm 0.1$ for $U/\gamma = 0.06$ and $\eta = 1.7 \pm 0.2$ for $U/\gamma = 0.15$ (see the Appendix).

The phase transition observed here in 2D lattices is reminiscent of what predicted analytically in the driven-dissipative Bose-Hubbard model through an approximation where only the $k = 0$ mode is retained [9]. Therefore, one may expect that a macroscopic population in the $k = 0$ mode would always give rise to a critical behavior. In this regard, we studied the fraction $f_0 = n_{k=0}/n_{tot}$ of bosons in the $k = 0$ mode, where $n_{k=0}$ is the steady-state population of the driven $k = 0$ mode and n_{tot} is the total lattice population. In Figs. 4(a) and 4(b) we report the finite-size analysis of f_0 as a function of F. In the region of mean-field bistability, f_0 presents a minimum in both one and two dimensions. In one dimension this minimum saturates to a finite value as one approaches the thermodynamic limit, while in 2D f_0 exhibits a behavior consistent with a finite jump at the critical point. For the considered interaction, in both cases the population of the driven mode is dominant (f_0 close to 1), showing that the fluctuations induced by the coupling to nonzero-momentum modes destroy the critical behavior in one dimension.

Finally, we present the local equal-time second-order correlation function $g_0^{(2)} = \langle \hat{a}_j^\dagger \hat{a}_j^\dagger \hat{a}_j \hat{a}_j \rangle / \langle \hat{a}_j^\dagger \hat{a}_j \rangle^2$ as a function of F. This quantity describes the amplitude of the fluctuations in the field and has been employed extensively to investigate critical behavior in optical systems. In one dimension this quantity has a broad peak whose shape is shown to converge for large enough L [Fig. 4(c)], while in two dimensions [Fig. 4(d)] the
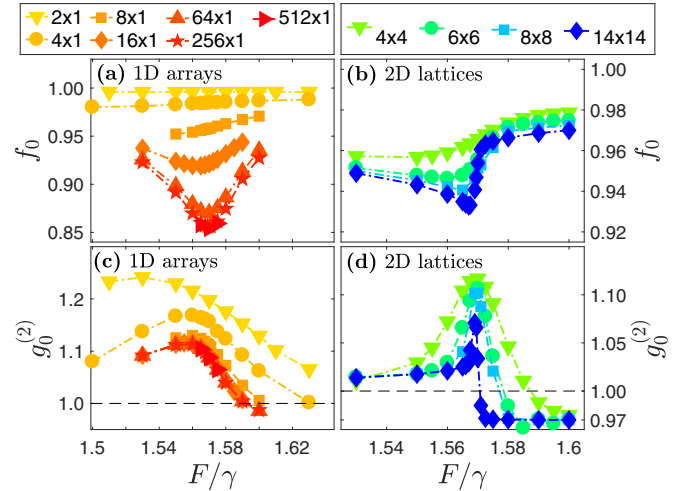

FIG. 4. (a) and (b) Population fraction $f_0 = n_{k=0}/n_{tot}$ in the zero-momentum mode as a function of the driving amplitude. (c) and (d) Zero-delay local second-order correlation $g_0^{(2)}$ versus F. Left panels are for 1D arrays, right panels for 2D lattices. The parameters are the same as in Fig. 1.

finite-size results show an emerging singular behavior in its derivative at the critical point. The same qualitative behavior is also observed in the large population limit of a single-mode nonlinear resonator [7,9], which is equivalent to the $k = 0$ approximation described above.

IV. CONCLUSIONS

In conclusion, we have theoretically predicted the critical slowing down associated with a dissipative transition in the driven-dissipative Bose-Hubbard model. We have revealed the emergence of critical dynamics in 2D lattices via a finite-size analysis, which is instead absent in 1D arrays, indicating that the lower critical dimension for this nonequilibrium model is $d < 2$. We have shown that in 1D arrays fluctuations destroy criticality of the dynamics even if the driven mode is macroscopically occupied. The asymptotic
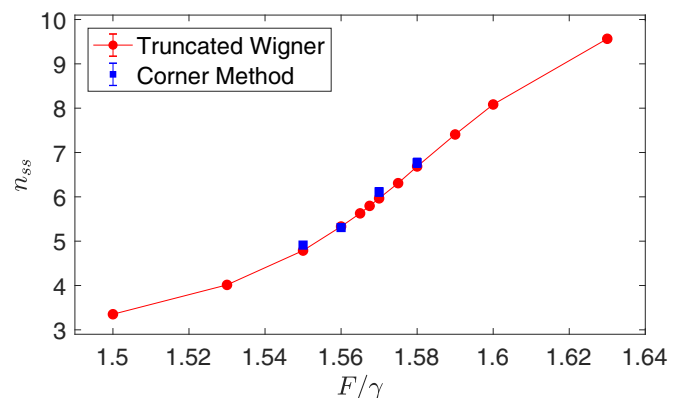

FIG. 5. Steady-state average boson occupation per site as a function of the driving F/γ in a 4×1 array. Different symbols correspond to different numerical methods. The statistical error is of the order of the symbol size. The parameters are $U/\gamma = 0.1$, $zJ/\gamma = 0.9$, and $\Delta/\gamma = 0.1$.
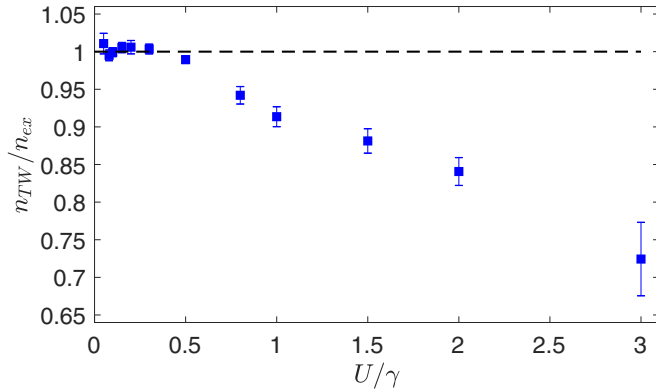
FIG. 6. Ratio between the steady-state average occupation obtained through the truncated Wigner approximation n_{TW} and the exact Runge-Kutta integration of the Lindblad master equation n_{ex} in a 2×1 array. The error bars refer to the statistical noise of the results associated with the stochastic Langevin simulations. Here F/γ has been varied so that $U F^2/\gamma^3 = 2.465$ is kept constant; $z J/\gamma = 0.9$ and $\Delta/\gamma = 0.1$ are fixed. Note that the results for $U/\gamma \leqslant 0.2$ have been obtained with the corner-space renormalization.

FIG. 7. Minimum of the Liouvillian gap λ as a function of the size L of 2D lattices, for different values of U/γ. The critical exponent is $\eta = 1.7 \pm 0.2$ for $U/\gamma = 0.15$, $\eta = 3.3 \pm 0.1$ for $U/\gamma = 0.1$, and $\eta = 5.3 \pm 0.1$ for $U/\gamma = 0.06$. The parameters are $z J/\gamma = 0.9$ and $\Delta/\gamma = 0.1$.

decay rate associated with the Liouvillian frequency gap has been measured in nonlinear photonic systems with different techniques [28,30,31], hence the critical slowing down predicted here as a function of lattice size is within experimental reach and can unveil fundamental properties of dissipative phase transitions. Many intriguing studies can be foreseen on the horizon, including the role of disorder as well as the critical behavior of exotic open photonic lattices with geometric frustration [46–49] or quasiperiodicity [25,50].

ACKNOWLEDGMENTS

APPENDIX: BENCHMARK OF THE TRUNCATED WIGNER APPROXIMATION

In this appendix we present numerical results showing that the truncated Wigner approximation is accurate in the regime of parameters considered in the paper. To do so, we compare its results to what was obtained with numerically exact methods for small systems. Moreover, we show how the power-law
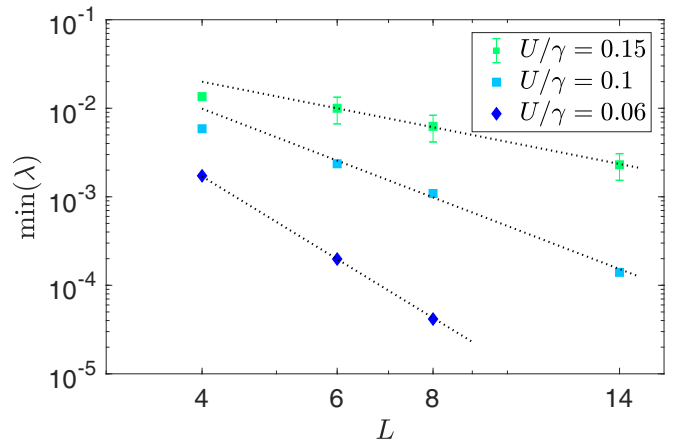
decay of the Liouvillian gap changes when the normalized interaction U/γ is varied.

In Fig. 5 we present the steady-state average population in a 4×1 array computed with the truncated Wigner approximation and with the corner-space renormalization method [40], finding excellent agreement between the two. The values considered are the same as in the main text. We would like to point out that for the considered value of $U/\gamma = 0.1$, a brute-force integration of the master equation for a one-site system requires a cutoff of $N_{\max} = 40$ bosons in order to achieve adequate numerical convergence. In a 4×1 lattice the required dimension of the Hilbert space would be $40^4 = 2.56 \times 10^6$, which cannot be handled numerically without more advanced methods. For the parameters considered in the main text, this lattice can still be tackled by the corner-space renormalization method (going to larger lattice sizes would require significantly larger computational resources).

In Fig. 6 we present the ratio $n_{\mathrm{TW}}/n_{\mathrm{ex}}$ between the steady-state average population obtained via the truncated Wigner approximation n_{TW} and exact methods n_{ex} as a function of the nonlinearity U/γ. We used this quantity to identify the range of values in U/γ for which the truncated Wigner approximation is quantitatively accurate, finding that for $U/\gamma \leqslant 0.3$ the truncated Wigner approximation yields results within 1% of the exact value.

In Fig. 7 we present the minimum of the Liouvillian gap λ as a function of lattice size L for several 2D lattices with different nonlinearities. We find that the power-law exponent increases as U/γ is decreased.

[1] S. Sachdev, *Quantum Phase Transitions* (Cambridge University Press, Cambridge, 2001).

[2] H. Breuer and F. Petruccione, *The Theory of Open Quantum Systems* (Oxford University Press, Oxford, 2007).

[3] E. M. Kessler, G. Giedke, A. Imamoglu, S. F. Yelin, M. D. Lukin, and J. I. Cirac, Phys. Rev. A **86**, 012116 (2012).

[4] H. J. Carmichael, Phys. Rev. X **5**, 031028 (2015).

[5] J. J. Mendoza-Arenas, S. R. Clark, S. Felicetti, G. Romero, E. Solano, D. G. Angelakis, and D. Jaksch, Phys. Rev. A **93**, 023821 (2016).

[6] W. Casteels, F. Storme, A. Le Boité, and C. Ciuti, Phys. Rev. A **93**, 033824 (2016).

[7] N. Bartolo, F. Minganti, W. Casteels, and C. Ciuti, Phys. Rev. A **94**, 033841 (2016).

[8] W. Casteels and C. Ciuti, Phys. Rev. A **95**, 013812 (2017).

[9] W. Casteels, R. Fazio, and C. Ciuti, Phys. Rev. A **95**, 012128 (2017).

[10] M. Foss-Feig, P. Niroula, J. T. Young, M. Hafezi, A. V. Gorshkov, R. M. Wilson, and M. F. Maghrebi, Phys. Rev. A **95**, 043826 (2017).

[11] M. Biondi, G. Blatter, H. E. Türeci, and S. Schmidt, Phys. Rev. A **96**, 043809 (2017).

[12] A. Biella, F. Storme, J. Lebreuilly, D. Rossini, R. Fazio, I. Carusotto, and C. Ciuti, Phys. Rev. A **96**, 023839 (2017).

[13] V. Savona, Phys. Rev. A **96**, 033826 (2017).

[14] L. M. Sieberer, S. D. Huber, E. Altman, and S. Diehl, Phys. Rev. Lett. **110**, 195301 (2013).

[15] L. M. Sieberer, S. D. Huber, E. Altman, and S. Diehl, Phys. Rev. B **89**, 134310 (2014).

[16] E. Altman, L. M. Sieberer, L. Chen, S. Diehl, and J. Toner, Phys. Rev. X **5**, 011017 (2015).

[17] T. E. Lee, S. Gopalakrishnan, and M. D. Lukin, Phys. Rev. Lett. **110**, 257204 (2013).

[18] J. Jin, A. Biella, O. Viyuela, L. Mazza, J. Keeling, R. Fazio, and D. Rossini, Phys. Rev. X **6**, 031011 (2016).

[19] M. F. Maghrebi and A. V. Gorshkov, Phys. Rev. B **93**, 014307 (2016).

[20] R. Rota, F. Storme, N. Bartolo, R. Fazio, and C. Ciuti, Phys. Rev. B **95**, 134431 (2017).

[21] A. Kshetrimayum, H. Weimer, and R. Orús, Nat. Commun. **8**, 1291 (2017).

[22] I. Carusotto and C. Ciuti, Rev. Mod. Phys. **85**, 299 (2013).

[23] C. Noh and D. G. Angelakis, Rep. Prog. Phys. **80**, 016401 (2017).

[24] M. J. Hartmann, J. Opt. **18**, 104005 (2016).

[25] A. Amo and J. Bloch, C. R. Phys. **17**, 934 (2016).

[26] T. Jacqmin, I. Carusotto, I. Sagnes, M. Abbarchi, D. D. Solnyshkov, G. Malpuech, E. Galopin, A. Lemaître, J. Bloch, and A. Amo, Phys. Rev. Lett. **112**, 116402 (2014).

[27] A. A. Houck, H. E. Tureci, and J. Koch, Nat. Phys. **8**, 292 (2012).

[28] M. Fitzpatrick, N. M. Sundaresan, A. C. Y. Li, J. Koch, and A. A. Houck, Phys. Rev. X **7**, 011016 (2017).

[29] R. Labouvie, B. Santra, S. Heun, and H. Ott, Phys. Rev. Lett. **116**, 235302 (2016).

[30] S. R. K. Rodriguez, W. Casteels, F. Storme, N. Carlon Zambon, I. Sagnes, L. Le Gratiet, E. Galopin, A. Lemaître, A. Amo, C. Ciuti, and J. Bloch, Phys. Rev. Lett. **118**, 247402 (2017).

[31] T. Fink, A. Schade, S. Höfling, C. Schneider, and A. İmamoğlu, Nat. Phys. (2017), doi:10.1038/s41567-017-0020-9.

[32] J. M. Fink, A. Dombi, A. Vukics, A. Wallraff, and P. Domokos, Phys. Rev. X **7**, 011012 (2017).

[33] V. V. Albert and L. Jiang, Phys. Rev. A **89**, 022118 (2014).

[34] K. Vogel and H. Risken, Phys. Rev. A **39**, 4675 (1989).

[35] I. Carusotto and C. Ciuti, Phys. Rev. B **72**, 125335 (2005).

[36] H. Carmichael, *Statistical Methods in Quantum Optics 1: Master Equations and Fokker-Planck Equations*, Physics and Astronomy Online Library (Springer, Berlin, 1998).

[37] C. Rackauckas and Q. Nie, Discrete Cont. Dyn. Syst. B **22**, 2731 (2017).

[38] A. Le Boité, G. Orso, and C. Ciuti, Phys. Rev. A **90**, 063821 (2014).

[39] A. Le Boité, G. Orso, and C. Ciuti, Phys. Rev. Lett. **110**, 233601 (2013).

[40] S. Finazzi, A. Le Boité, F. Storme, A. Baksic, and C. Ciuti, Phys. Rev. Lett. **115**, 080604 (2015).

[41] P. D. Drummond and D. F. Walls, J. Phys. A: Math. Gen. **13**, 725 (1980).

[42] R. M. Wilson, K. W. Mahmud, A. Hu, A. V. Gorshkov, M. Hafezi, and M. Foss-Feig, Phys. Rev. A **94**, 033801 (2016).

[43] P. Drummond and M. Hillery, *The Quantum Theory of Nonlinear Optics* (Cambridge University Press, Cambridge, 2014).

[44] H. Wiseman and G. Milburn, *Quantum Measurement and Control* (Cambridge University Press, Cambridge, 2010).

[45] C. Gardiner and P. Zoller, *Quantum Noise: A Handbook of Markovian and Non-Markovian Quantum Stochastic Methods with Applications to Quantum Optics*, Springer Series in Synergetics Vol. 56 (Springer, Berlin, 2004).

[46] S. Mukherjee, A. Spracklen, D. Choudhury, N. Goldman, P. Öhberg, E. Andersson, and R. R. Thomson, Phys. Rev. Lett. **114**, 245504 (2015).

[47] F. Baboux, L. Ge, T. Jacqmin, M. Biondi, E. Galopin, A. Lemaître, L. Le Gratiet, I. Sagnes, S. Schmidt, H. E. Türeci, A. Amo, and J. Bloch, Phys. Rev. Lett. **116**, 066402 (2016).

[48] W. Casteels, R. Rota, F. Storme, and C. Ciuti, Phys. Rev. A **93**, 043833 (2016).

[49] M. Biondi, E. P. L. van Nieuwenburg, G. Blatter, S. D. Huber, and S. Schmidt, Phys. Rev. Lett. **115**, 143601 (2015).

[50] D. Tanese, E. Gurevich, F. Baboux, T. Jacqmin, A. Lemaître, E. Galopin, I. Sagnes, A. Amo, J. Bloch, and E. Akkermans, Phys. Rev. Lett. **112**, 146404 (2014).